HL-LHC INNER TRIPLET POWERING AND CONTROL STRATEGY

S. Yammine, H. Thiesen, CERN, Geneva, Switzerland

Abstract

In order to achieve the target 3000 fb^{-1} integrated field for the HL-LHC (High Luminosity – Large Hadron Collider) at ATLAS and CMS, new large aperture quadrupoles are required for the final focusing triplet magnets before the interaction points. These low-β magnets, based on the Nb_3Sn technology, deliver a peak field of 11.4 T. They consist of two outer quadrupoles, Q1 and Q3 and a central one divided into two identical magnets, Q2a and Q2b. To optimize the powering and the beam dynamics of these triplets, the quadrupoles will be powered in series by a single high-current two quadrants (2-Q) converter [18 kA, ±10 V]. Three 4-Q trim power converters are added over Q1 [±2 kA, ±10 V], Q2a [±0.12 kA, ±10 V] and Q3 [±2 kA, ±10 V] to account for possible transfer function difference between the quadrupoles. This paper presents the powering scheme of the four mentioned coupled circuits. A digital control strategy, using four standard LHC digital controllers, to decouple the four systems and to achieve a high precision control is proposed and discussed.

INTRODUCTION

The inner triplet circuit provides the final focusing of the proton beams before collision at four locations in the LHC. For the HL-LHC requirements, the inner triplet magnets at the interaction regions IR1 (ATLAS) and IR5 (CMS) will be upgraded with larger aperture magnets, to allow for the increase of the β* with a larger field gradient [1]. Each inner triplet consists of three quadrupole optical elements and four magnets (Q1, Q2a, Q2b and Q3). Q1 and Q3 are identical magnets (MQXFA magnet) developed in the USA. Q2a and Q2b are identical magnets (MQXFB magnet) developed at CERN. In this paper, the powering and the control strategies of the inner triplet magnets circuit are discussed.

CIRCUIT LAYOUT

One circuit will be used to feed the HL-LHC inner triplet main circuits at points 1 and 5, as was done for the LHC [2]. The magnets Q1, Q2a, Q2b and Q3 of type MQXF will be powered in series by a main power converter that delivers up to 18 kA as shown in Figure 1. This main power converter is bidirectional in voltage, to be able to ramp-down the current in the circuit fast enough to respect the operation requirements. Two trims will be added over Q1 and Q3 of rating [±2 kA/±10 V] to be able to compensate up to 11 % of the transfer function difference between the magnets. One trim will be added over Q2a for K-modulation purposes.

Table 1: Inner Triplet Main Circuit Parameters

Circuit	Magnet Type	Nominal Current [kA]	Ultimate Current [kA]	Inductance [mH]	Cable Resistance [mΩ]
Triplet (Q1, Q2a, Q2b, Q3)	MQXFA / MQFXB	16.5	17.82	255	0.26
Trim Q1	MQXFA	±2	±2	69	1.44
Trim Q3	MQXFA	±2	±2	69	1.44
Trim Q2a	MQXFB	±0.12	±0.12	58.5	13.4
Q2b	MQXFB			58.5	

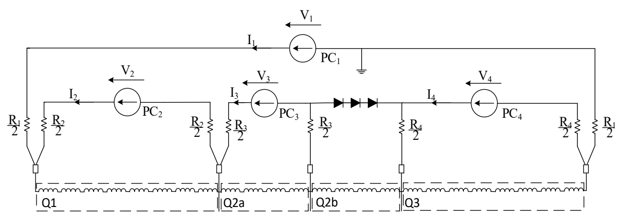

Figure 1: Inner triplet main circuit layout.

CONTROL STRATEGY

High precision is a necessary requirement in current control for the LHC main circuits [3]. A current error less than 1 ppm with respect to the ultimate circuit current for the inner triplet circuit is required. The HL-LHC inner triplet circuit is a nested circuit with four power converters as shown on Figure 1. This introduces coupling of the different sub-circuits, or, in other terms, a variation in one sub-circuit would lead to a variation in current in other circuits during transients. In order to reach a high precision of the current, the proposed control strategy is to decouple every sub-circuit using decoupling matrices and to reduce the interaction between these sub-circuits as was proposed in [4].

HL-LHC Inner Triplet Main Circuit Model

The state equations that describe the interaction between the sub-circuits of the inner triplet circuit are the following:

$$\dot{X} = AX + BU$$

Where

$$X = \begin{bmatrix} I_1 \\ I_2 \\ I_3 \\ I_4 \end{bmatrix};\ U = \begin{bmatrix} V_1 \\ V_2 \\ V_3 \\ V_4 \end{bmatrix}$$

$$A = \frac{1}{L_{2b}} \begin{bmatrix} -R_1 & R_2 & R_3 & R_4 \\ R_1 & -R_2\left(1+\frac{L_{2b}}{L_1}\right) & -R_3 & -R_4 \\ R_1 & -R_2 & -R_3\left(1+\frac{L_{2b}}{L_{2a}}\right) & -R_4 \\ R_1 & -R_2 & -R_3 & -R_2\left(1+\frac{L_{2b}}{L_3}\right) \end{bmatrix}$$

$$B = \frac{1}{L_{2b}}\begin{bmatrix} 1 & -1 & -1 & -1 \\ -1 & \left(1+\frac{L_{2b}}{L_1}\right) & 1 & 1 \\ -1 & 1 & \left(1+\frac{L_{2b}}{L_{2a}}\right) & 1 \\ -1 & 1 & 1 & \left(1+\frac{L_{2b}}{L_3}\right) \end{bmatrix}$$

Circuit Decoupling Method

In order to decouple the sub-systems, two decoupling matrices are applied in order to transform the system from a MIMO (4x4) system to four SISO equivalent systems. The decoupling matrices (K and D) are applied to the system input as follows:

$$\begin{aligned} \dot{X} &= AX + B(KX + DW) \\ &= (A + BK)X + (BD)W \\ &= A_d X + B_d W \end{aligned}$$

Where

$$A_d = \begin{bmatrix} -\frac{R_1}{L_{TOT}} & 0 & 0 & 0 \\ 0 & -\frac{R_2}{L_1} & 0 & 0 \\ 0 & 0 & -\frac{R_3}{L_{2a}} & 0 \\ 0 & 0 & 0 & -\frac{R_4}{L_3} \end{bmatrix} \quad B_d = \begin{bmatrix} \frac{1}{L_{TOT}} & 0 & 0 & 0 \\ 0 & \frac{1}{L_1} & 0 & 0 \\ 0 & 0 & \frac{1}{L_{2a}} & 0 \\ 0 & 0 & 0 & \frac{1}{L_3} \end{bmatrix}$$

L_{TOT} is the total inductance of the inner triplet main circuit. Therefore, the decoupling matrices are calculated as follows:

$$K = B^{-1}\,(A_d - A) \text{ and } D = B^{-1}\,(B_d)$$

Matrices K and D are therefore defined as the following:

$$K = \begin{bmatrix} 0 & -R_2 & -R_3 & -R_4 \\ -\frac{R_1 L_1}{L_{TOT}} & 0 & 0 & 0 \\ -\frac{R_1 L_{2a}}{L_{TOT}} & 0 & 0 & 0 \\ -\frac{R_1 L_3}{L_{TOT}} & 0 & 0 & 0 \end{bmatrix} \qquad D = \begin{bmatrix} 1 & 1 & 1 & 1 \\ \frac{L_1}{L_{TOT}} & 1 & 0 & 0 \\ \frac{L_{2a}}{L_{TOT}} & 0 & 1 & 0 \\ \frac{L_3}{L_{TOT}} & 0 & 0 & 1 \end{bmatrix}$$

RST Controller Synthesis for Independent Current Control

One RST controller is applied to each decoupled circuit. The transfer function of each decoupled circuit could be written as the following in the discrete domain:

$$H(z) = \frac{B(z)}{A(z)} = \frac{b_1}{z + a_1}$$

$$a_1 = -e^{\frac{-T_s}{\tau}};\ b_1 = K\left(1 - e^{\frac{-T_s}{\tau}}\right)$$

$$K = \frac{1}{R}\ ;\ \tau = \frac{L}{R}$$

T_s represents the sampling period of the control process. Its value should be wisely chosen between a minimum period that respects Shannon's frequency with a safe margin and a maximum value that avoids the issues due to the digital oversampling and the precision requirements. In [5], the selection criteria is defined as the following:

$$6f_b \le \frac{1}{T_s} \le 25 f_b$$

where f_b is the required bandwidth frequency of the system in closed loop. The RST implementation is shown on Figure 2 for each decoupled circuit and is detailed in [6]. Two integrators are added in the RST to assure a zero tracking error. In addition, the RST controller parameters are determined to provide a dead-beat controller of d+1 cycles of delay where d is the delay introduced by the control and measurement process in terms of time cycles (i.e. the sampling period). f_b is hence defined as the noise rejection capability of the controller and is in the order of 1Hz for the inner triplet circuit.

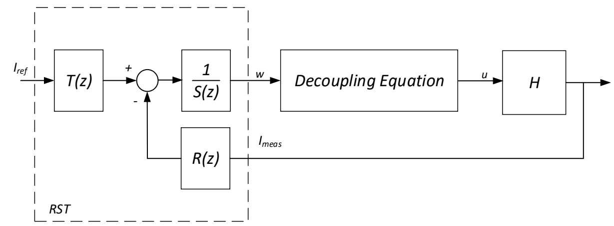

Figure 2: RST controller implementation for the each decoupled circuit.

Decoupling Controller Implementation

The Function Generator/Controller (FGC) is the component that performs the controller computations [7]. In contrast with the LHC inner triplet circuit where the decoupling matrix is implemented on an analogue card [4], the HL-LHC inner triplet decoupling matrix will be implemented by means of equations on the FGC, hence a digital decoupling will be used. After the RST is computed, the output values of the RST and the measured currents should be communicated between the FGCs in order to compute the decoupling equations. The decoupling matrices show that information sharing is present between {PC1 and PC2}, {PC1 and PC3} and {PC1 and PC4}. Figure 3 shows the architecture of the decoupling control for the inner triplet main circuit. Raw Ethernet communication will be used in order to share the information between the FGCs. Using interrupt signals, the data could be sent from one FGC to another with a delay of less than 0.1 ms (refer to Figure 4). This delay is acceptable for the inner triplet control since the sampling period is in the order of 100 ms.

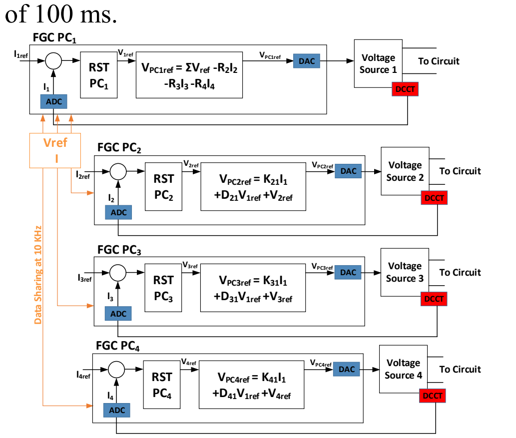

Figure 3: Decoupling control architecture.

ISBN 978-3-95450-182-3

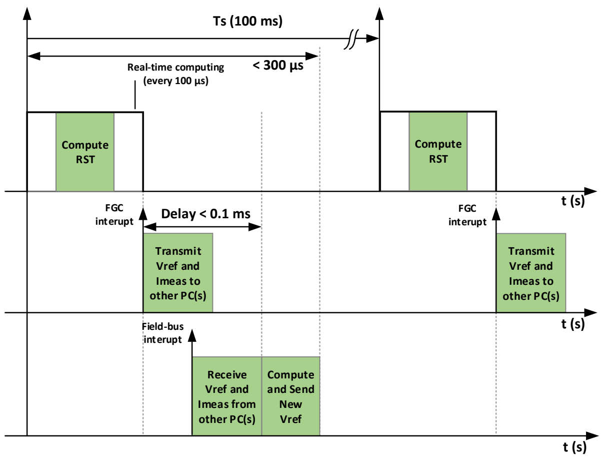

Figure 4: Timeline of events in one FGC controller.

Simulation Results

The presented model of the inner triplet circuit, the RST and the decoupling controller are simulated using Matlab/Simulink ®. In the simulations, the delay d is considered as one sampling time cycle in the model. Figure 5 shows the current control following a PLP (Parabolic Linear Parabolic) reference used in the LHC up till the ultimate current for the main current and trim Q1 and Q3. The simulated currents are shown for demonstration reasons. It should be noted that the addition of currents should not exceed the ultimate current in the magnets (in contrast with the shown currents for Q1). In addition, a ΔL/L and a ΔR/R of ±10% or ±20% are applied in order to show the robustness against magnet saturation and cable resistance variations.

Figure 6 shows the main reference current and the simulated current in linear ramp-up zone. As expected from the dead-beat control strategy, a time delay of two sampling periods is seen. Figure 7 shows that the error between the reference current (with 2 sampling periods delay) and the current in the four circuits is less than 0.06 part per million (ppm) with respect to the ultimate current for ΔL/L and a ΔR/R of ±10% and less than 0.15 ppm for ΔL/L and a ΔR/R of ±20%. This result is satisfactory since a precision of less than 1 ppm is desired from the circuit control and measurement.

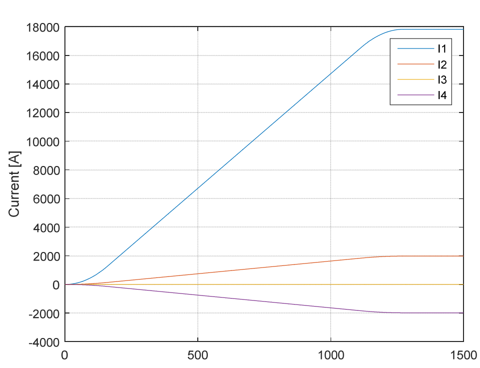

Figure 5: Current response of the RST + decoupling control with a PLP curve reference till ultimate current for I1 and sinusoidal reference for I2 and I4.

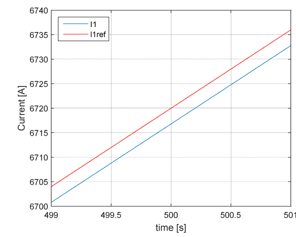

Figure 6: Zoom on the main reference current and simulated current show a time delay of two sampling periods.

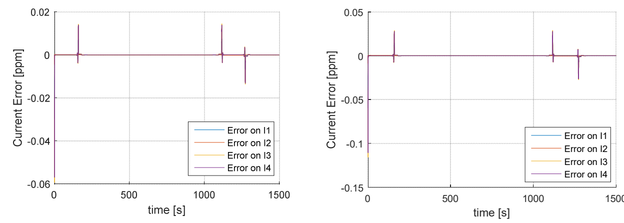

(a) (b)

Figure 7: Error in ppm with respect to the ultimate current between the reference currents and the currents in the circuits for: (a) ΔL/L and a ΔR/R of ±10% and (b) ΔL/L and a ΔR/R of ±20%.

CONCLUSION

This paper describes the circuit layout to power the new magnets of the HL-LHC inner triplet which consists of a nested circuit. The presented control strategy is based on the LHC strategy and consists of an RST control combined with a decoupling matrix implemented digitally. Simulations show satisfactory results and a high precision control.

ACKNOWLEDGEMENT

Acknowledgments are due to Q. King, M. Martino and all members of the HL-LHC Magnet Circuit Forum and TE-EPC involved in the work described for all the ideas and information they provided.

REFERENCES

[1] High-Luminosity Large Hadron Collider (HL-LHC) Technical Design Report V.01, Geneva, 2017.
[2] LHC Design Report, Geneva, 2004.
[3] H. Thiesen, M. C. Bastos, G. Hudson, Q. King, V. Montabonnet, D. Nisbet and S. Page, "High Precision Current Control," in *Proc. IPAC'10*, Kyoto, Japan, 2010.
[4] F. Bordry and H. Thiesen, "LHC Inner Triplet Powering Strategy," in *Proc. NA-PAC'10*, Chicago, USA, 2010.
[5] I. D. Landau, Identification et Commade des Systèmes, Hermès, 1993.
[6] F. Bordry and H. Thiesen, "RST Digital Algorithm for Controlling the LHC Magnet Current," EP2 Forum, ESRF, Grenoble France, 1998.
[7] Q. King, "The All-Digital Approach to LHC Power Converter Current Control," in *Proc. ICALEPCS'09*, Kobe, Japan, 2009.